



ORIGINAL ARTICLE

# Topological optimization of composite trusses considering CO<sub>2</sub> emission via metaheuristics algorithms

*Otimização topológica de treliças mistas considerando a emissão de CO<sub>2</sub> por meio de algoritmos meta-heurísticos*

Gabriel Erlacher<sup>a</sup> Adenilcia Fernanda Grobério Calenzani<sup>a</sup> Élcio Cassimiro Alves<sup>a</sup> <sup>a</sup>Universidade Federal do Espírito Santo – UFES, Departamento de Engenharia Civil, Vitória, ES, Brasil

Received 28 November 2022

Accepted 05 February 2023

**Abstract:** In order to provide more sustainable solutions to the design of composite truss beams, the present work proposes a formulation to optimize dimensional, geometric and topologic parameters aiming to minimize CO<sub>2</sub> emissions. Genetic Algorithm (GA) and Particle Swarm Optimization (PSO) are used to solve the optimization problem considering the choice of steel profiles, characteristic strength of concrete, formwork, number of panels and truss total height. The methodology is applied to three problems where three different types of profile geometry and three models of truss are considered in order to compare and analyze its results. The program considers double angles, circular hollow tubes and circular concrete-filled tubes, as well as Pratt, Howe and Warren models. The three problems are identical, with the exception of the span size, varying between 8, 24 and 40 meters. In conclusion, results show the algorithms provide equal or similar solutions, with the Warren model and circular concrete-filled tube being the best solutions in all cases, especially for larger spans, reaching an emission reduction of up to 40% in relation to the Howe model using double angles. The critical criterion in the sizing of all cases attained a design-resistant effort relation greater than 90% in all cases, confirming the effectiveness of the optimization, being the combined criterion the critical in most of them.

**Keywords:** optimization, composite truss, meta-heuristic algorithm, environmental impact, topological optimization.

**Resumo:** A fim de fornecer soluções mais sustentáveis para o projeto de vigas mistas treliçadas, o presente trabalho propõe uma formulação para otimizar parâmetros dimensionais, geométricos e topológicos visando minimizar as emissões de CO<sub>2</sub>. Algoritmo Genético (GA) e Otimização por Enxame de Partículas (PSO) são utilizados para resolver o problema de otimização considerando a escolha dos perfis de aço, resistência característica do concreto, formas, número de painéis e altura total da treliça. A metodologia é aplicada a três problemas onde são considerados três tipos diferentes de geometria de perfil e três modelos de treliça para comparar e analisar seus resultados. O programa considera cantoneiras duplas, tubos circulares vazados e tubos circulares preenchidos com concreto, bem como os modelos de treliça Pratt, Howe e Warren. Os três problemas são idênticos, com exceção do tamanho do vão, que varia entre 8, 24 e 40 metros. Em conclusão, os resultados mostram que os algoritmos fornecem soluções iguais ou semelhantes, sendo o modelo de Warren e o tubo circular preenchido com concreto o mais eficiente em todos os casos, especialmente para vãos maiores, atingindo uma redução de emissão de até 40% em relação ao modelo Howe utilizando cantoneiras duplas. O critério crítico no dimensionamento de todos os casos atingiu uma relação entre esforço solicitante e resistente maior que 90% em todos os casos, confirmando a eficácia da otimização, sendo o critério de flexão combinada o crítico na maioria deles.

**Palavras-chave:** otimização, viga mista, algoritmo meta-heurístico, impacto ambiental, otimização topológica.

**How to cite:** G. Erlacher, A. F. G. Calenzani, and E. C. Alves, "Topological optimization of composite trusses considering CO<sub>2</sub> emission via metaheuristics algorithms," *Rev. IBRACON Estrut. Mater.*, vol. 16, no. 6, e16606, 2023, <https://doi.org/10.1590/S1983-41952023000600006>

**Corresponding author:** Élcio Cassimiro Alves. E-mail: [elcio.calves1@email.com](mailto:elcio.calves1@email.com)

**Financial support:** The authors acknowledge the Brazilian Federal Government Agency CAPES for the financial support provided during the development of this research. The second author thanks the Brazilian Federal Government Agency CNPq for the productivity research grant number 309741/2020-3.

**Conflict of interest:** Nothing to declare.

**Data Availability:** Data-sharing is not applicable to this article as no new data were created or analyzed in this study.



This is an Open Access article distributed under the terms of the Creative Commons Attribution License, which permits unrestricted use, distribution, and reproduction in any medium, provided the original work is properly cited.

## 1 INTRODUCTION

Reducing greenhouse gas emissions is one of the greatest challenges on this century [1]. The IPCC's Sixth Assessment Report estimates that the emission of greenhouse gases from human activities is responsible for approximately 1.1°C of warming compared to pre-industrial levels and it is expected to reach or exceed 1.5°C of warming [2]. In 2020, even though the economic activity was severely reduced due to the pandemic, building construction demand for steel and cement was still responsible for 3.2 gigatons of CO<sub>2</sub> in energy-related emissions and, thereby, contributing with 10% of global carbon emissions [3]. Therefore, it is essential that actions are taken in favor of decreasing greenhouse gas emissions and avoiding even more consequences that arise from global warming.

Many studies have pointed to structural optimization as an option to reduce environmental impact, as it allows a more efficient and rational use of construction materials [4]–[11]. This is mainly because the current dimensioning method is usually done by trial-and-error, making the solution's efficiency depend on the designer's experience or at the expense of laborious manual adjustment work [12]. In this way, with the structural optimization, it is possible to obtain the combination of parameters that minimizes the impact caused by the construction, which makes the process more practical and the structure more efficient while still meeting security conditions [13].

Different methodologies have been employed to measure the environmental impact of buildings, among them the Life Cycle Assessment (LCA), which is a method that studies the environmental inputs and outputs related to a product or service life-cycle from its production until the end of its service life [14]. A parameter that is often used to account for this impact on structural optimization of various structures is the CO<sub>2</sub> emission, as done by Payá-Zaforteza et al. [4], García-Segura and Yepes [15] and Santoro and Kripka [16].

Recent studies have been using several different algorithms in the structural optimization, such as Genetic Algorithms (GA) and Particle Swarm Optimization (PSO). GA was first proposed by John Holland and is based on Darwin's theory of evolution: it starts with an initial population of solutions to the problem and, in each generation, crossings are made from the most fit individuals and mutations are added, simulating natural selection and resulting, in the end, in the best solution to the problem [10]. PSO, on the other hand, was first proposed by Kennedy, Eberhart and Shi and it is based on a population of solutions, called particles, which are classified according to their fitness. Then, each particle is accelerated towards the best particle and also towards their own best previously found solution. In each iteration, particles approach the best solution from a different direction and will very likely find a position, that is, a solution that is better than the initial one, creating a new best solution to be followed in the next iteration. The optimization is finished when the maximum number of iterations is reached [17].

Several studies have used GA and PSO to optimize a large range of structures, such as reinforced concrete [18]–[20], composite beams [21]–[23], composite cellular beams [24]–[25], steel trusses [26]–[28], steel endplate semi-rigid joints [29], etc. However, the topological optimization of composite truss beams considering environmental impact is yet to be undertaken.

Composite trusses are structures composed of a steel truss united by shear connectors to a concrete slab. The consideration of the concrete slab as a compressive resistant element provides a significant increase to the flexural strength of the beam, since, in general, about 50% of the weight of a truss arises from the compressed flange [30]. In this way, composite truss beam presents itself as an economical option, especially in situations where it is necessary to overcome spans greater than 20 meters [31]. Another advantage of composite trusses is the fact that they are relatively light and allow the passage of complex electrical, ventilating and communication systems, while still overcoming building height limitations or allowing the construction of higher beams, which minimizes deflection and vibrations [32], [33].

The composite slab is composed of a metallic formwork covered with a layer of concrete and a reinforcing mesh to absorb concrete's retraction stresses on its upper part. The shape of the truss can consist of different types of profiles, such as tubular, double angles brackets, etc. and follow different assembly models, like Pratt, Howe and Warren.

Multiple factors can influence the distribution of forces in each bar of a truss, such as dimensions, geometry and topology. Consequently, performing an optimization of these parameters can significantly decrease the weight of the structure, as it allows for a better exploitation of the material. Dimensional optimization refers to the consideration of the structure's dimensions as variables, such as profile shapes; geometric optimization considers the position of each element as a variable, such as the position of the nodes; and the topological optimization considers the parameters that change the quantity and distribution of elements as a variable. Studies, such as Kaveh and Ahmadi's [34] and Tarabay and Lima [35], indicated that the best solutions are found in the simultaneous optimization of these three parameters and Müller and van der Klashorst [36] corroborate them, showing an average economy of 22% in comparison to the dimensional-only optimization.

Therefore, the present work proposes the formulation of the dimensional and topological optimization problem of a composite steel-concrete truss beam, considering the current safety verifications and aiming to find the solution that causes minimum environmental impact, through different metaheuristic algorithms - GA and PSO. The algorithm is applied to different combinations of truss models and profile shapes, allowing the comparison between solutions and a

conclusion on what is the most efficient combination of steel profiles, concrete resistance, formwork and truss topology. The dimensional optimization is done by varying the profile used in each element of the truss and the topological optimization is achieved by varying the number of elements, as well as their positions.

## 2 OPTIMIZATION PROBLEM FORMULATION

### 2.1 Design Variables

Figure 1 presents the design variables considered by the program in the optimization.

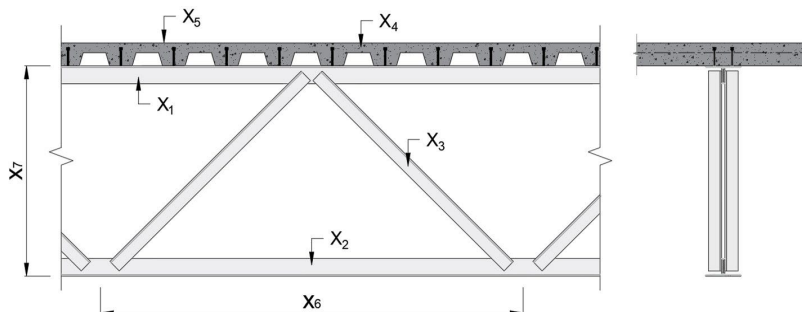


Figure 1. Design variables.

Where  $x(1)$  is the upper chord profile;  $x(2)$  is the lower chord profile;  $x(3)$  is the web Members profile;  $x(4)$  is the characteristic strength of the concrete slab ( $f_{ck}$ );  $x(5)$  is the decking profile;  $x(6)$  is the number of panels in the truss; and  $x(7)$  is the Truss height.

When using double angles (DA) and circular hollow tubes (CHT), the program considers seven variables, but when using circular concrete-filled tubes (CCFT) an eighth variable is considered. This variable is identified as  $x(8)$  and represents the characteristic strength of the concrete infill.

### 2.2 Search Range

The lower and upper bounds to each variable are presented by Equation 1 and Equation 2, respectively.

$$LB = \{1, 1, 1, 1, 1, L/15, 1\} \tag{1}$$

$$UP = \{N, N, N, 7, 48, 2L, L/8, 7\} \tag{2}$$

Where the first three elements of each vector represent the number of available profile choices according to the catalogs used,  $N$  being 50, for double angles [37], and 142, for tubular profiles [38]; The fourth element represents the variation of the slab  $f_{ck}$ , varying between 20, 25, 30, 35, 40, 45 and 50MPa; The fifth element refers to the number of choices of formwork available in the catalog used [39], which in this case were 48; The sixth element represents the maximum number of truss panels, which for Pratt and Howe trusses must be an even number to ensure symmetry. The minimum size for a panel was 500 mm, thus making the maximum number of panels two times the total span ( $L$ ). The seventh element represents the number of options for the height of the truss, taken arbitrarily as values between one fifteenth and one eighth of the span, varying from 50 to 50 mm. The eighth element is only relevant when using CCFT profile and represents the compressive strength of the filling concrete, as considered for the fourth element.

### 2.3 Objective Function

The objective function proposed in this work refers to the minimization of the  $CO_2$  emission of composite trusses and it is presented in Equation 3.

$$E_{total} = E_s + E_c + E_f + E_m + E_{sc} + E_{cf} \tag{3}$$

Where  $E_{total}$  corresponds to the total emission of CO<sub>2</sub> caused by the composite truss.  $E_s$ ,  $E_c$ ,  $E_f$ ,  $E_m$ ,  $E_{sc}$  and  $E_{cf}$  correspond to the emission caused by the production of steel profiles, concrete used in the slab, steel formwork, reinforcing mesh, shear connectors and concrete fill, respectively. When using DA or CHT,  $E_{cf}$  is null.

The way in which each of these variables is calculated is expressed by Equation 4 to 9.

$$E_s = (m_p + m_{cn}) \times U_s \tag{4}$$

$$E_c = V_{c,u} \times e \times L \times U_c \tag{5}$$

$$E_f = m_{f,u} \times e \times L \times U_f \tag{6}$$

$$E_m = m_{m,u} \times e \times L \times U_m \tag{7}$$

$$E_{sc} = n_{sc} \times m_{sc,u} \times U_s \tag{8}$$

$$E_{cf} = A_{cf} \times L \times U_{cf} \tag{9}$$

Where  $m_p$  is the total mass of steel profiles;  $m_{cn}$  is the mass of connections, estimated as 10% of the mass of profiles;  $U_s$  is the unitary emission of CO<sub>2</sub> per unit of steel mass;  $V_{c,u}$  is the volume of concrete per unit of slab area, given in function of the formwork’s geometry;  $e$  is the distance between beams;  $L$  is the span;  $U_c$  is the unitary emission of CO<sub>2</sub> per unit of concrete volume, given in function of its resistance;  $m_{f,u}$  is the mass of steel formwork per unit of slab area, given in function of the formwork width;  $U_f$  is the unitary emission of CO<sub>2</sub> per unit of steel formwork mass;  $m_{m,u}$  is the mass of reinforcing mesh per unit of slab area, given in function of the slab’s width [39];  $U_m$  is the unitary emission of CO<sub>2</sub> per unit of reinforcing mesh mass;  $n_{sc}$  is the number of shear connectors used in the whole beam;  $m_{sc,u}$  is the mass of one shear connector;  $A_{cf}$  is the internal area of the upper chord profile (CCFT); and, similarly to  $U_c$ ,  $U_{cf}$  is the unitary emission of CO<sub>2</sub> per unit of volume of filling concrete.

The unitary emissions used in the program and their sources are exhibited in Table 1.

**Table 1** – Unitary emissions.

| Material                      | CO <sub>2</sub> Emission                 | Source                      |
|-------------------------------|--|-----------------------------|
| Concrete ( $f_{ck} = 20$ MPa) | 140.05 kgCO <sub>2</sub> /m <sup>3</sup> | Santoro and Kripka [16]     |
| Concrete ( $f_{ck} = 25$ MPa) | 149.26 kgCO <sub>2</sub> /m <sup>3</sup> |                             |
| Concrete ( $f_{ck} = 30$ MPa) | 157.65 kgCO <sub>2</sub> /m <sup>3</sup> |                             |
| Concrete ( $f_{ck} = 35$ MPa) | 171.64 kgCO <sub>2</sub> /m <sup>3</sup> |                             |
| Concrete ( $f_{ck} = 40$ MPa) | 182.14 kgCO <sub>2</sub> /m <sup>3</sup> |                             |
| Concrete ( $f_{ck} = 45$ MPa) | 194.70 kgCO <sub>2</sub> /m <sup>3</sup> |                             |
| Concrete ( $f_{ck} = 50$ MPa) | 225.78 kgCO <sub>2</sub> /m <sup>3</sup> |                             |
| Steel Profile (VMB350)        | 1.12 kgCO <sub>2</sub> /kg               | Worldsteel Association [40] |
| Steel Formwork [39]           | 2.64 kgCO <sub>2</sub> /kg               |                             |
| Reinforcing Mesh (CA60)       | 1.92 kgCO <sub>2</sub> /kg               |                             |
| Stud Bolt (ø19mm, 105mm)      | 0.23 kgCO <sub>2</sub> /unit             |                             |

The CO<sub>2</sub> emissions of each material were defined based on the Life Cycle Assessment (LCA) methodology. The method consists of analyzing all the constructive stages of the material: extraction, production, transport, use, maintenance and also the end of the life cycle, represented by the stages of demolition, landfill or reuse.

## 2.4 Security Constraints

In order to be valid, a solution must follow the criteria of ultimate limit states (ULS) and serviceability limit states (SLS) prescribed by the current Brazilian standards [41], [42], which is done by the constraints presented in Equations 10 to 22.

$$C(1): \frac{N_{Sd,bs,ac}}{N_{c,Rd}} - 1 \leq 0 \quad (10)$$

$$C(2): \frac{N_{Sd,bs,dc}}{N_{c,Rd}} - 1 \leq 0 \quad (11)$$

$$C(3): \frac{N_{Sd,bi,ac}}{N_{t,Rd}} - 1 \leq 0 \quad (12)$$

$$C(4): \frac{N_{Sd,bi,dc}}{N_{t,Rd}} - 1 \leq 0 \quad (13)$$

$$C(5): \frac{N_{Sd,dm,ac}}{N_{c,Rd}} - 1 \leq 0 \quad (14)$$

$$C(6): \frac{N_{Sd,dm,dc}}{N_{c,Rd}} - 1 \leq 0 \quad (15)$$

$$C(7): \frac{M_{Sd,mista}}{M_{Rd}} - 1 \leq 0 \quad (16)$$

$$\begin{cases} \text{if } \frac{N_{Sd,ac}}{N_{Rd}} \geq 0.2 \Rightarrow C(8): \frac{N_{Sd,ac}}{N_{Rd}} + \frac{8 M_{Sd,ac}}{9 M_{Rd}} - 1 \leq 0 \\ \text{if } \frac{N_{Sd,ac}}{N_{Rd}} < 0.2 \Rightarrow C(8): \frac{N_{Sd,ac}}{2 N_{Rd}} + \frac{M_{Sd,ac}}{M_{Rd}} - 1 \leq 0 \end{cases} \quad (17)$$

$$\begin{cases} \text{if } \frac{N_{Sd,dc}}{N_{Rd}} \geq 0.2 \Rightarrow C(9): \frac{N_{Sd,dc}}{N_{Rd}} + \frac{8 M_{Sd,dc}}{9 M_{Rd}} - 1 \leq 0 \\ \text{if } \frac{N_{Sd,dc}}{N_{Rd}} < 0.2 \Rightarrow C(9): \frac{N_{Sd,dc}}{2 N_{Rd}} + \frac{M_{Sd,dc}}{M_{Rd}} - 1 \leq 0 \end{cases} \quad (18)$$

$$C(10): \frac{\delta_0}{\delta_{Adm}} - 1 \leq 0 \quad (19)$$

$$C(11): \frac{\delta_{Total}}{\delta_{Adm}} - 1 \leq 0 \quad (20)$$

$$C(12): \frac{n_{total,cs}}{n_{max,cs}} - 1 \leq 0 \quad (21)$$

Where  $C(1)$  and  $C(2)$  refers to the limitation on the upper chord's axial loading before and after curing, respectively;  $C(3)$  and  $C(4)$  refers to the limitation on the lower chord's axial loading before and after curing, respectively;  $C(5)$  and  $C(6)$  refers to the limitation on the web members' axial loading before and after curing, respectively;  $C(7)$  refers to the limitation on the composite section's bending moment;  $C(8)$  and  $C(9)$  refers to the limitation on the combined bending on the upper chord before and after curing, respectively;  $C(10)$  and  $C(11)$  refers to the limitation of deflection before and after curing; and  $C(12)$  refers to a verification on the number of shear connectors, in order to make sure the spacing between them is higher than the criteria established by current standards [41].

Aiming to solve the optimization problem proposed, the program uses Matlab's native Genetic Algorithm. As for the PSO, it was implemented in Matlab with the Adaptive Penalty Method (APM) proposed by Lemonge and Barbosa [27]. For the PSO, a population of one hundred individuals was considered, 75 iteration steps and a tolerance of  $10^{-6}$  as a stopping

criterion and solution convergence. For GA, the initial population contains 120 individuals, the rate of elite individuals and crossing of the intermediate type are 0.05 and 0.8, respectively, whereas the mutation rate is random.

### 3. RESULTS AND DISCUSSIONS

In order to compare the algorithms, truss models and profile shapes, the developed program was applied to three composite beams, with identical materials and loading conditions, and span lengths of 8, 24 and 40 meters. In each case, Genetic Algorithm (GA) and Particle Swarm Optimization (PSO) were used to optimize each combination between truss model – Pratt, Howe and Warren – and profile geometry – Double Angle (DA), Circular Hollow Tube (CHT) and Circular Concrete-Filled Tube (CCFT) – obtaining 18 solutions for each problem. In all of them, the following loading conditions were considered: live load of 2 kN/m<sup>2</sup>, live or fixed partitions of 1 kN/m<sup>2</sup> and floor coverings of 0.15 kN/m<sup>2</sup>. The other loads, due to self-weight, are calculated according to the elements chosen by the solution and the combinations of actions considered according to Brazilian standards [43]. The concrete used is produced with gneiss aggregate and the composite slab has ribs parallel to the beams, which are spaced 2 meters apart and shored before curing. It was also considered that the steel has a modulus of elasticity of 200 GPa and the modulus of rupture of the connectors’ steel is 450 MPa. The yield strength of the steel is 355 MPa to the profiles, 600 MPa to the reinforcing mesh and 280 MPa to the formwork.

#### 3.1 Truss with 8 meters

The first situation analyzed is a composite truss with a span of 8 meters. All solutions pointed to the same slab characteristics: 20 MPa concrete, 110 mm of width, thickness of 0.8 mm, rib of 50 mm and reinforcement mesh composed of bars of 3.8mm diameter, spaced from 150 to 150 mm. Consequently, the emission due to the slab was the same, equal to 190.47 kg for concrete, 354.13 kg for the formwork and 186.24 for the reinforcement mesh. It is important to note that 20MPa was the minimum permissible resistance to the concrete and the choice of shape was also the minimum emission. The convergence between solutions can be explained by the constancy of loading conditions and spacing between beams. In addition, the results corroborate the work of Santoro and Kripka [16], who concluded that, in reinforced concrete elements submitted to bending moment, it is more advantageous to use concrete with lower compressive strengths when considering only CO<sub>2</sub> emissions. However, it is important to mention that the evaluation the durability of the structural element could lead to different results, as the increase of concrete’s compressive resistance also provides a gain of durability.

The number of connectors also remained the same, most likely due to the constancy of the slab configurations. The strength of a connector depends on the slab and shear connectors parameters. As both remained constant, the resistance of a connector also continued the same. The number of shear connectors, on the other hand, depends on two criteria: bearing stress on the slab concrete and the yield of the connector steel. Because the slab conditions also remained constant and the concrete bearing stress criterion was critical in all cases, the number of connectors remained constant in all solutions. The solution indicated 17 connectors, generating an emission of 4.43 kgCO<sub>2</sub> and totaling 586.28 kgCO<sub>2</sub>. The emission due to steel profiles and concrete filling, however, varied from case to case and is presented in Table 2.

**Table 2.** CO<sub>2</sub> emission of each solution to the 8-m truss.

| Truss Model | Profile Shape | Truss Model | Profile Shape |         | TOTAL* |
|-------------|---------------|-------------|---------------|---------|--------|
|             |               |             | PROFILE       | FILLING |        |
| Pratt       | DA            | GA          | 178.48        | -       | 764.75 |
|             |               | PSO         | 178.48        | -       | 764.75 |
|             | CHT           | GA          | 133.43        | -       | 719.70 |
|             |               | PSO         | 133.43        | -       | 719.70 |
|             | CCFT          | GA          | 90.90         | 1.14    | 677.18 |
|             |               | PSO         | 90.90         | 1.14    | 677.18 |
| Howe        | DA            | GA          | 185.48        | -       | 771.76 |
|             |               | PSO         | 185.48        | -       | 771.76 |
|             | CHT           | GA          | 137.29        | -       | 723.57 |
|             |               | PSO         | 137.29        | -       | 723.57 |
|             | CCFT          | GA          | 108.33        | 0.69    | 695.30 |
|             |               | PSO         | 108.33        | 0.69    | 695.30 |
| Warren      | DA            | GA          | 171.48        | -       | 757.75 |
|             |               | PSO         | 171.48        | -       | 757.75 |
|             | CHT           | GA          | 130.36        | -       | 716.63 |
|             |               | PSO         | 130.36        | -       | 716.63 |
|             | CCFT          | GA          | 87.66         | 0.79    | 674.73 |
|             |               | PSO         | 87.66         | 0.79    | 674.73 |

\*The total emission is the sum of the emission from the profiles, filling, and slab.

As can be seen in Table 2, both algorithms converged to the same solution in all cases, confirming its accuracy. The solution that presented the best result was the Warren truss using CCFT and the worst solution was obtained in the Howe truss using DA, causing 14.4% more emission, as shown in Figure 2, where the total emission of each solution is compared to the best solution. In general, the solutions given by DA were the least efficient, generating, on average, 11.8% more CO<sub>2</sub> than CCFT solutions. It is also noted that solutions using CHT are, on average, 5.4% less efficient than the solution of the same model using CCFT, reinforcing the relevance of this structural element. Table 3 presents the geometric properties of each solution, and Figure 3 presents the best solutions to each truss model, as well as the best solution using DA.

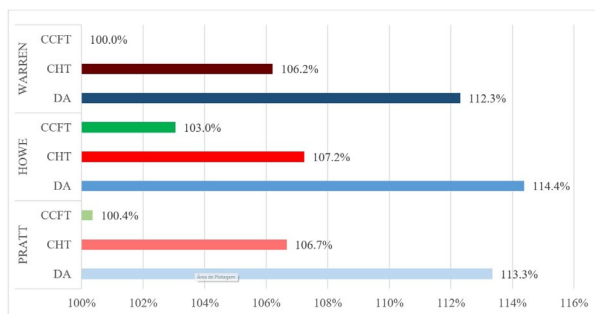


Figure 2. Comparison between solutions provided to the 8-m truss.

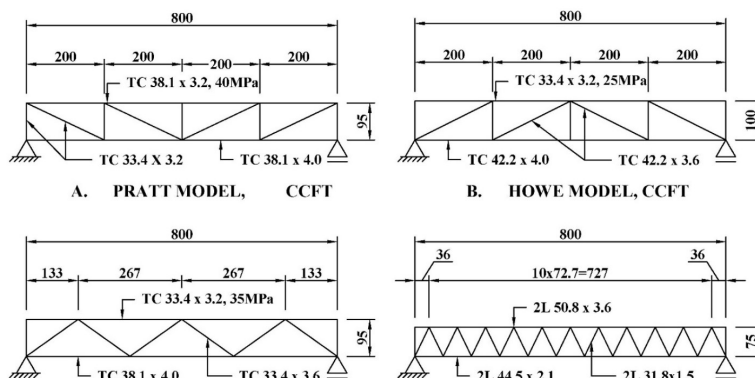


Figure 3. Final geometry of the best solutions to the eight meters truss.

Table 3. Geometric parameters of solutions provided to the 8-m truss.

| Truss Model | Profile Shape | Alg. | Lower Chord   | Upper Chord   | Web Members   | N° Panels | Height [mm] | Filling f <sub>ck</sub> [MPa] |
|-------------|---------------|------|---------------|---------------|---------------|-----------|-------------|-------------------------------|
| Pratt       | DA            | GA   | 2L 38.1 x 1.8 | 2L 50.8 x 3.6 | 2L 38.1 x 1.8 | 12        | 800         | -                             |
|             |               | PSO  | 2L 38.1 x 1.8 | 2L 50.8 x 3.6 | 2L 38.1 x 1.8 | 12        | 800         | -                             |
|             | CHT           | GA   | TC 42.2 x 4.0 | TC 60.3 x 4.0 | TC 33.4 x 3.2 | 8         | 900         | -                             |
|             |               | PSO  | TC 42.2 x 4.0 | TC 60.3 x 4.0 | TC 33.4 x 3.2 | 8         | 900         | -                             |
|             | CCFT          | GA   | TC 38.1 x 4.0 | TC 38.1 x 3.2 | TC 33.4 x 3.2 | 4         | 950         | 40                            |
|             |               | PSO  | TC 38.1 x 4.0 | TC 38.1 x 3.2 | TC 33.4 x 3.2 | 4         | 950         | 40                            |
| Howe        | DA            | GA   | 2L 44.5 x 2.1 | 2L 50.8 x 3.6 | 2L 38.1 x 1.8 | 11        | 750         | -                             |
|             |               | PSO  | 2L 44.5 x 2.1 | 2L 50.8 x 3.6 | 2L 38.1 x 1.8 | 11        | 750         | -                             |
|             | CHT           | GA   | TC 42.2 x 4.0 | TC 60.3 x 4.0 | TC 33.4 x 3.2 | 8         | 1000        | -                             |
|             |               | PSO  | TC 42.2 x 4.0 | TC 60.3 x 4.0 | TC 33.4 x 3.2 | 8         | 1000        | -                             |
|             | CCFT          | GA   | TC 42.2 x 4.0 | TC 33.4 x 3.2 | TC 42.2 x 3.6 | 4         | 1000        | 25                            |
|             |               | PSO  | TC 42.2 x 4.0 | TC 33.4 x 3.2 | TC 42.2 x 3.6 | 4         | 1000        | 25                            |
| Warren      | DA            | GA   | 2L 44.5 x 2.1 | 2L 50.8 x 3.6 | 2L 31.8 x 1.5 | 11        | 750         | -                             |
|             |               | PSO  | 2L 44.5 x 2.1 | 2L 50.8 x 3.6 | 2L 31.8 x 1.5 | 11        | 750         | -                             |
|             | CHT           | GA   | TC 38.1 x 4.0 | TC 73.0 x 3.6 | TC 33.4 x 3.2 | 6         | 1000        | -                             |
|             |               | PSO  | TC 38.1 x 4.0 | TC 73.0 x 3.6 | TC 33.4 x 3.2 | 6         | 1000        | -                             |
|             | CCFT          | GA   | TC 38.1 x 4.0 | TC 33.4 x 3.2 | TC 33.4 x 3.6 | 3         | 950         | 35                            |
|             |               | PSO  | TC 38.1 x 4.0 | TC 33.4 x 3.2 | TC 33.4 x 3.6 | 3         | 950         | 35                            |

It can be noted by the analysis of the Table that the trusses constituted by DA have lower heights and a higher number of panels than the others. This is because, compared to CHT profiles and especially to CCFT, DA profiles are slender, which restricts the size of the elements. The filling of tubular profiles significantly increases the stiffness of the elements, making the upper chord more resistant to compression. This resistance gain allows reducing considerably the steel area of the upper chord profiles and also increasing its length, allowing larger panels. The increase in emission caused by the concrete used in the filling of the profiles is insignificant when compared to the emission avoided by the reduction of the steel area, as shown in Table 2 and in accordance with the work by Guimarães et al. [44] and Lourenço et al. [45]. Figure 4 shows the emission composition of each solution.

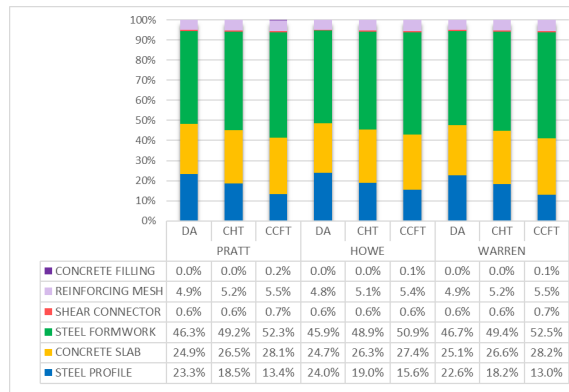


Figure 4. CO<sub>2</sub> Emission Composition of solutions provided to the 8-m truss.

Figure 4 confirms that the emission due to the concrete used in filling the upper chords represents 0.1% to 0.2% of the total emission, while the emission of steel reduces from 3.4% to 5.2% only by filling the profiles. In the cases analyzed, the steel formwork was the largest responsible for the emission, generating more than 45% of the emissions, followed by the concrete slab, with more than 24%. Figure 5 shows which constraints predominated in the optimization problem and Table 4 shows the relation between design and resistant efforts.

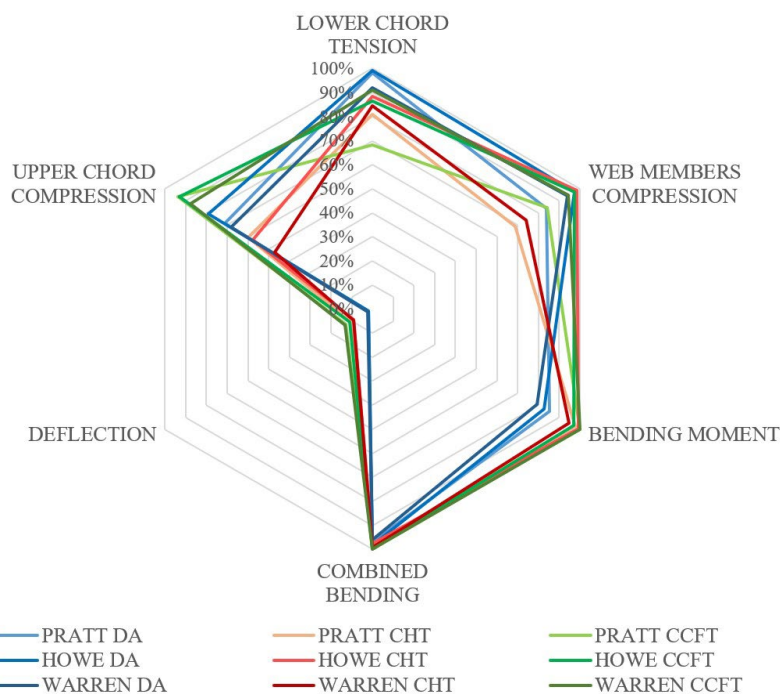


Figure 5. Constraints analysis provided to the 8-m truss.

**Table 4.** Relation between design and resistant efforts of the solutions.

| Truss Model | Profile Shape | Upper Chord Compression | Lower Chord Tension | Web Members Compression | Bending Moment | Combined Bending | Deflection |
|-------------|---------------|-------------------------|---------------------|-------------------------|----------------|------------------|------------|
| Pratt       | DA            | 71.05%                  | <b>98.06%</b>       | 83.74%                  | 85.17%         | 96.80%           | 1.78%      |
|             | CHT           | 59.70%                  | 80.90%              | 68.98%                  | 97.61%         | <b>99.92%</b>    | 10.53%     |
|             | CCFT          | 93.60%                  | 68.30%              | 84.04%                  | <b>99.85%</b>  | 98.59%           | 12.83%     |
| Howe        | DA            | 79.22%                  | <b>99.24%</b>       | 97.40%                  | 82.87%         | 98.14%           | 1.95%      |
|             | CHT           | 57.44%                  | 88.56%              | 98.60%                  | <b>99.24%</b>  | 97.66%           | 9.09%      |
|             | CCFT          | 93.11%                  | 86.41%              | 97.26%                  | 96.83%         | <b>99.90%</b>    | 11.03%     |
| Warren      | DA            | 68.13%                  | 92.01%              | 94.04%                  | 79.28%         | <b>96.07%</b>    | 2.35%      |
|             | CHT           | 47.17%                  | 84.41%              | 74.16%                  | 95.77%         | <b>99.36%</b>    | 9.22%      |
|             | CCFT          | 87.79%                  | 90.96%              | 94.44%                  | <b>99.80%</b>  | 99.75%           | 13.31%     |

As shown in Table 4, the lower chord tension criterion was critical only for solutions using DA, while the bending moment was more restrictive for the others, reaching more than 95% and being the critical in three of them. For all solutions, the combined bending was a very expressive criterion, reaching more than 95% and proving to be a significant criterion on the sizing of composite trusses. This criterion evaluates the upper chord's ability to resist the combination of compression and bending moment. The resistance gain and consequent CO<sub>2</sub> emission reduction could be explained by the fact that the concrete filling considerably reduces the dimension of the profile used in the upper chord without losing its resistant capacity.

### 3.2 Truss with 24 meters

In the second example, a 24-meter-long truss with the same slab configurations as the previous example is analyzed. The emission of concrete slab, formwork and reinforcing mesh increased to 571.40, 1062.38 and 111.75 kgCO<sub>2</sub>, respectively, proportionally to the span growth. The number of connectors also increased to 50 connectors, representing an emission of 13.04 kgCO<sub>2</sub> and totaling 1745.53 kgCO<sub>2</sub>.

The emission due to the steel profiles and the concrete filling of the upper chords is shown in Table 5, where it can be noted that the algorithms diverged in most cases, but provided solutions with total emissions that differ by less than 2% from one another. Only in one case the GA led to a more efficient solution than the PSO; in two cases there was convergence and; in six, the PSO obtained the best solutions, indicating a greater efficiency of the algorithm for this type of problem. Table 6 shows the geometric characteristics for the final solutions of the optimization problem and Figure 6 presents the geometry of the best solutions to each truss model, as well as the best solution using DA.

**Table 5.** CO<sub>2</sub> emission of each solution to the 24-m truss.

| Truss Model | Profile Shape | Algorithm | CO <sub>2</sub> Emission (kgCO <sub>2</sub> ) |          |         |
|-------------|---------------|-----------|---|----------|---------|
|             |               |           | Profile                                       | Concrete | Total*  |
| Pratt       | DA            | GA        | 1934.18                                       | -        | 3692.75 |
|             |               | PSO       | 1934.18                                       | -        | 3692.75 |
|             | CHT           | GA        | 1211.26                                       | -        | 2969.83 |
|             |               | PSO       | 1194.85                                       | -        | 2953.42 |
|             | CCFT          | GA        | 824.49  | 18.95    | 2583.06 |
|             |               | PSO       | 810.56  | 15.50    | 2569.13 |
| Howe        | DA            | GA        | 1987.66                                       | -        | 3746.23 |
|             |               | PSO       | 1987.66                                       | -        | 3746.23 |
|             | CHT           | GA        | 1343.05                                       | -        | 3101.62 |
|             |               | PSO       | 1314.43                                       | -        | 3073.00 |
|             | CCFT          | GA        | 979.41  | 14.75    | 2752.73 |
|             |               | PSO       | 1000.35                                       | 14.05    | 2772.97 |
| Warren      | DA            | GA        | 1863.13                                       | -        | 3601.70 |
|             |               | PSO       | 1808.14                                       | -        | 3566.71 |
|             | CHT           | GA        | 1154.83                                       | -        | 2913.40 |
|             |               | PSO       | 1150.50                                       | -        | 2909.07 |
|             | CCFT          | GA        | 758.04  | 16.51    | 2533.12 |
|             |               | PSO       | 755.94  | 16.51    | 2531.02 |

\*The total emission is the sum of the emission from the profiles, filling, and slab.

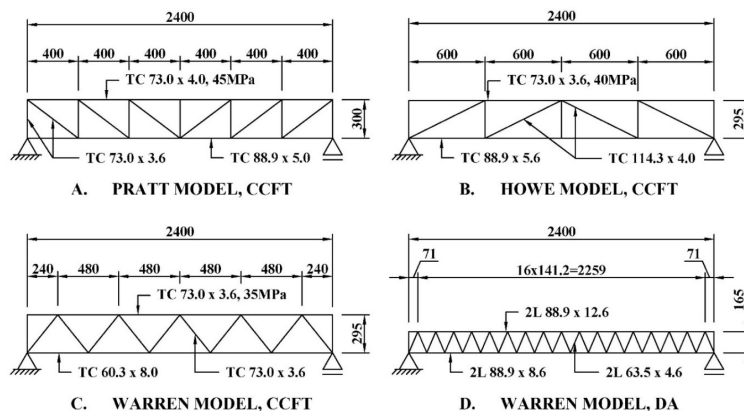


Figure 6. Final geometry to the best solutions to the 24-m truss.

Table 6. Geometric parameters of solutions provided to the 24-m truss.

| Truss Model | Profile Shape | Alg.          | Lower Chord    | Upper Chord     | Web Members    | N° Panels | Height [mm] | f <sub>ck</sub> [MPa] |
|-------------|---------------|---------------|----------------|-----------------|----------------|-----------|-------------|-----------------------|
| Pratt       | DA            | GA            | 2L 88.90 x 8.6 | 2L 101.6 x 14.6 | 2L 76.20 x 5.5 | 14        | 1600        | -                     |
|             |               | PSO           | 2L 88.90 x 8.6 | 2L 101.6 x 14.6 | 2L 76.20 x 5.5 | 14        | 1600        | -                     |
|             | CHT           | GA            | TC 101.6 x 5.0 | TC 141.3 x 5.6  | TC 73.0 x 3.6  | 8         | 2700        | -                     |
|             |               | PSO           | TC 60.3 x 8.8  | TC 141.3 x 5.0  | TC 73.0 x 3.6  | 10        | 2650        | -                     |
|             | CCFT          | GA            | TC 73.0 x 6.4  | TC 88.9 x 3.6   | TC 73.0 x 3.6  | 6         | 2850        | 25                    |
| Howe        | DA            | GA            | 2L 88.90 x 8.6 | 2L 88.90 x 12.6 | 2L 76.20 x 5.5 | 18        | 1650        | -                     |
|             |               | PSO           | 2L 88.90 x 8.6 | 2L 88.90 x 12.6 | 2L 76.20 x 5.5 | 18        | 1650        | -                     |
|             | CHT           | GA            | TC 73.0 x 8.0  | TC 141.3 x 5.0  | TC 73.0 x 4.5  | 10        | 2650        | -                     |
|             |               | PSO           | TC 73.0 x 7.1  | TC 141.3 x 5.6  | TC 88.9 x 3.6  | 8         | 2900        | -                     |
|             | CCFT          | GA            | TC 88.9 x 5.6  | TC 73.0 x 3.6   | TC 114.3 x 4.0 | 4         | 2950        | 40                    |
| Warren      | DA            | GA            | 2L 76.20 x 7.3 | 2L 101.6 x 14.6 | 2L 76.20 x 5.5 | 11        | 2000        | -                     |
|             |               | PSO           | 2L 88.90 x 8.6 | 2L 88.9 x 12.6  | 2L 63.50 x 4.6 | 17        | 1650        | -                     |
|             | CHT           | GA            | TC 88.9 x 5.0  | TC 114.3 x 5.6  | TC 60.3 x 4.0  | 11        | 3000        | -                     |
|             |               | PSO           | TC 60.3 x 8.8  | TC 141.3 x 5.0  | TC 60.3 x 4.0  | 10        | 2650        | -                     |
|             | CCFT          | GA            | TC 88.9 x 5.0  | TC 73.0 x 3.6   | TC 73.0 x 3.6  | 5         | 2950        | 35                    |
| PSO         | TC 60.3 x 8.0 | TC 73.0 x 3.6 | TC 73.0 x 3.6  | 5               | 2950           | 35        |             |                       |

According to Table 6, it is noticeable that trusses using DA have the lowest truss heights, as well as the highest number of panels, while the others presented similar and significantly higher heights. Once again, it is observed that most solutions using CCFT point to concretes with resistance greater than 35MPa, indicating that, for this purpose, concretes with higher strength are more effective. This is because, comparing the profiles used in the upper chords of CHT and CCFT solutions, there is a significant reduction in the dimensions of the profiles used. Figure 7 presents a comparison between each solution and the minimum emission, only being indicated the best solution found between GA and PSO, to each case.

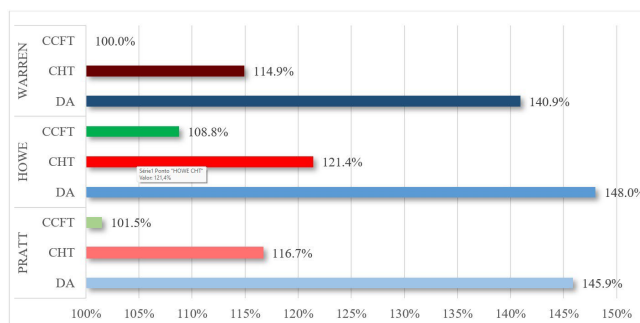


Figure 7. Comparison between solutions provided to the 24-m truss.

As in the previous example, the Warren model solution using CCFT was the most efficient and the Howe model using DA the least efficient, a difference even larger than the previous example, reaching 48.0%. The average difference between the solutions provided by the different profile geometries also increased, with the emission of the CHT being 14.37% higher and the DA 34.11% higher than the emission of the CCFT. This relative increase is justified by the greater expressiveness of the emission caused by steel profiles, as shown in Figure 8.

The largest emission for this example varied, being again the steel formwork in the trusses using CCFT and the steel profiles in the others, something that is justified by the greater difference between the emissions of each solution. The other elements have lost some expressiveness for this length of span. Figure 9 shows the constraints that governed the problem and Table 7 shows the proportions between design and resistant efforts of each case.

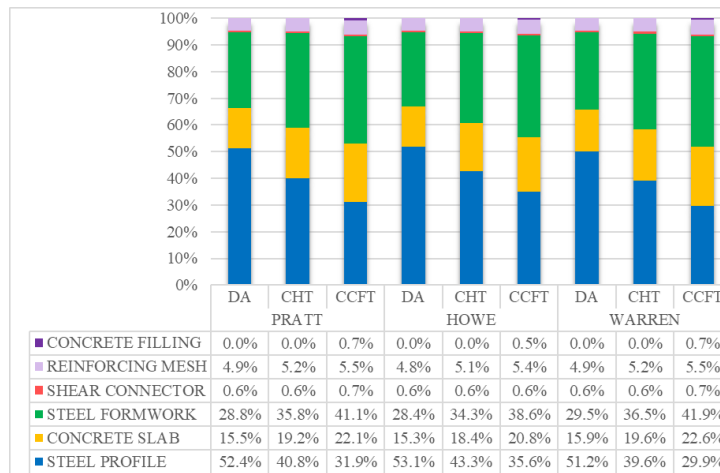


Figure 8. CO<sub>2</sub> Emission Composition of a 24-m span.

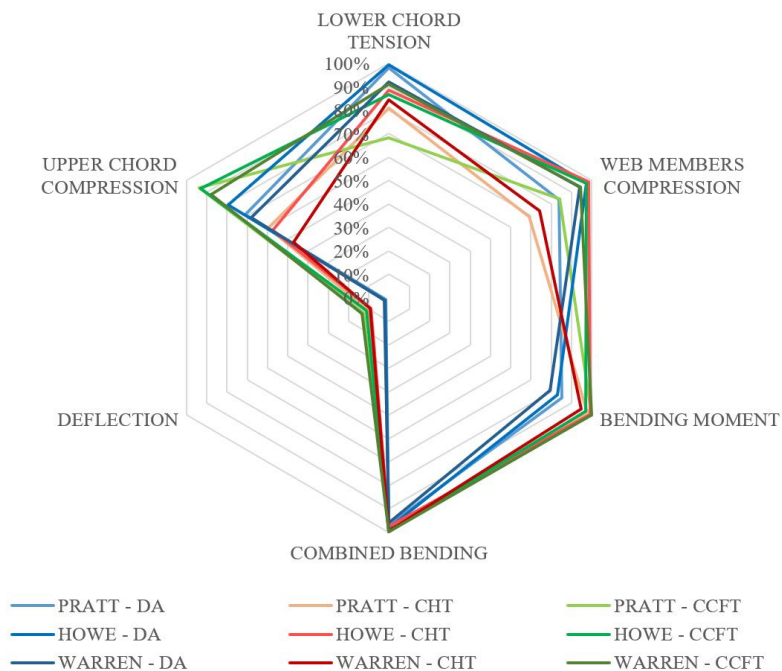


Figure 9. Constraints analysis provided to the 24 meters truss.

**Table 7.** Relation between design and resistant efforts of the solutions.

| Truss Model | Profile Shape | Upper Chord Compression | Lower Chord Tension | Web Members Compression | Bending Moment | Combined Bending | Deflection |
|-------------|---------------|-------------------------|---------------------|-------------------------|----------------|------------------|------------|
| Pratt       | DA            | 74.56%                  | <b>99.01%</b>       | 90.72%                  | 94.37%         | 94.53%           | 17.28%     |
|             | CHT           | 61.88%                  | 87.88%              | 85.68%                  | <b>99.11%</b>  | 93.55%           | 15.80%     |
|             | CCFT          | 95.98%                  | 76.33%              | 98.44%                  | 97.03%         | <b>99.92%</b>    | 16.47%     |
| Howe        | DA            | 80.50%                  | <b>98.56%</b>       | 96.53%                  | 91.89%         | 96.28%           | 20.72%     |
|             | CHT           | 53.20%                  | 89.59%              | 95.89%                  | <b>98.95%</b>  | 97.83%           | 13.44%     |
|             | CCFT          | 88.58%                  | 86.05%              | 94.92%                  | 97.79%         | <b>98.31%</b>    | 15.46%     |
| Warren      | DA            | 67.23%                  | 94.56%              | 92.69%                  | 89.08%         | <b>99.38%</b>    | 15.23%     |
|             | CHT           | 61.14%                  | 90.41%              | <b>99.07%</b>           | 98.94%         | 92.81%           | 15.80%     |
|             | CCFT          | 92.62%                  | 87.70%              | <b>99.91%</b>           | 97.25%         | 98.76%           | 17.00%     |

As can be observed, the lower chord tension criterion was more relevant in trusses using DA, being the critical for the Pratt and Howe models. The bending moment criterion, on the other hand, was more expressive for tubular profiles, being critical in Pratt and Howe trusses using CHT. In the case of Warren trusses using CHT and CCFT, the stress criterion in the diagonals and amounts was critical and, in the others, it was the combined bending criterion. As in the previous case, the constraints referring the serviceability limit state, the maximum deflection, is the one that least impacts on the final solution of the optimization problem for all analyzed solutions.

### 3.3 Truss with 40 meters

For the third example, a truss with 40 meters of span with the same slab characteristics of the previous examples was analyzed. Similarly, the same slab concrete, steel formwork and reinforcement mesh strength solutions were indicated, each of them emitting 952.34, 1770.63 and 186.24 kgCO<sub>2</sub>, respectively. 84 connectors were required, generating 21.91 kgCO<sub>2</sub> and totaling 2931.12 kgCO<sub>2</sub>. The emissions related to the steel profile and the concrete filling are presented in Table 8.

**Table 8.** Geometric parameters of solutions provided to the 40-m truss.

| Truss Model | Profile Shape | Algorithm | CO <sub>2</sub> Emission (kgCO <sub>2</sub> ) |          |         |
|-------------|---------------|-----------|---|----------|---------|
|             |               |           | Profile                                       | Concrete | Total*  |
| Pratt       | DA            | GA        | 6335.49                                       | -        | 9266.61 |
|             |               | PSO       | 6335.49                                       | -        | 9266.61 |
|             | CHT           | GA        | 3503.90                                       | -        | 6435.01 |
|             |               | PSO       | 3490.92                                       | -        | 6422.04 |
|             | CCFT          | GA        | 2294.48                                       | 69.12    | 5294.71 |
|             |               | PSO       | 2294.48                                       | 69.12    | 5294.71 |
| Howe        | DA            | GA        | 6346.21                                       | -        | 9277.33 |
|             |               | PSO       | 6346.21                                       | -        | 9277.33 |
|             | CHT           | GA        | 3962.27                                       | -        | 6893.39 |
|             |               | PSO       | 4000.82                                       | -        | 6931.94 |
|             | CCFT          | GA        | 2922.01                                       | 69.12    | 5922.25 |
|             |               | PSO       | 2912.22                                       | 64.66    | 5908.00 |
| Warren      | DA            | GA        | 5961.09                                       | -        | 8892.21 |
|             |               | PSO       | 5961.09                                       | -        | 8892.21 |
|             | CHT           | GA        | 3422.31                                       | -        | 6353.43 |
|             |               | PSO       | 3407.94                                       | -        | 6339.06 |
|             | CCFT          | GA        | 2243.29                                       | 54.92    | 5229.33 |
|             |               | PSO       | 2267.68                                       | 60.97    | 5259.76 |

\*The total emission is the sum of the emission from the profiles, filling, and slab.

Table 8 shows that algorithms diverged in most cases, but again for solutions with total emissions that differ by less than 1%. Of the five cases where there was no convergence, GA provided more efficient solutions in two cases and PSO in three, representing a slight advantage for this algorithm in this example. Table 9 shows the geometric parameters of the provided trusses and Figure 10 presents the geometry of the best solutions to each truss model, as well as the best solution using DA.

**Table 9.** Geometric parameters of solutions provided to the 40-m truss.

| Truss Model | Profile Shape | Alg. | Lower Chord     | Upper Chord     | Web Members     | N° Panels | Height [mm] | $f_{ck}$ [MPa] |
|-------------|---------------|------|-----------------|-----------------|-----------------|-----------|-------------|----------------|
| Pratt       | DA            | GA   | 2L 101.6 x 14.6 | 2L 152.4 x 29.2 | 2L 127.0 x 12.3 | 12        | 2800        | -              |
|             |               | PSO  | 2L 101.6 x 14.6 | 2L 152.4 x 29.2 | 2L 127.0 x 12.3 | 12        | 2800        | -              |
|             | CHT           | GA   | TC 114.3 x 7.1  | TC 219.1 x 6.4  | TC 101.6 x 4.5  | 8         | 4700        | -              |
|             |               | PSO  | TC 114.3 x 8.0  | TC 168.3 x 7.1  | TC 101.6 x 4.0  | 12        | 4250        | -              |
|             | CCFT          | GA   | TC 101.6 x 8.0  | TC 114.3 x 4.0  | TC 114.3 x 4.0  | 6         | 4600        | 45             |
|             |               | PSO  | TC 101.6 x 8.0  | TC 114.3 x 4.0  | TC 114.3 x 4.0  | 6         | 4600        | 45             |
| Howe        | DA            | GA   | 2L 101.6 x 12.2 | 2L 127.0 x 23.5 | 2L 127.0 x 12.3 | 16        | 3300        | -              |
|             |               | PSO  | 2L 101.6 x 12.2 | 2L 127.0 x 23.5 | 2L 127.0 x 12.3 | 16        | 3300        | -              |
|             | CHT           | GA   | TC 101.6 x 10.0 | TC 168.3 x 7.1  | TC 114.3 x 4.5  | 12        | 4450        | -              |
|             |               | PSO  | TC 141.3 x 7.1  | TC 168.3 x 7.1  | TC 114.3 x 4.5  | 12        | 4450        | -              |
|             | CCFT          | GA   | TC 101.6 x 8.8  | TC 114.3 x 4.0  | TC 141.3 x 5.0  | 6         | 4700        | 45             |
|             |               | PSO  | TC 101.6 x 8.8  | TC 114.3 x 4.0  | TC 141.3 x 5.0  | 6         | 4650        | 40             |
| Warren      | DA            | GA   | 2L 127.0 x 15.3 | 2L 152.4 x 29.2 | 2L 101.6 x 9.8  | 13        | 2700        | -              |
|             |               | PSO  | 2L 127.0 x 15.3 | 2L 152.4 x 29.2 | 2L 101.6 x 9.8  | 13        | 2700        | -              |
|             | CHT           | GA   | TC 114.3 x 7.1  | TC 168.3 x 7.1  | TC 101.6 x 4.0  | 11        | 4750        | -              |
|             |               | PSO  | TC 114.3 x 7.1  | TC 168.3 x 6.4  | TC 101.6 x 4.0  | 12        | 4800        | -              |
|             | CCFT          | GA   | TC 114.3 x 6.4  | TC 114.3 x 4.5  | TC 114.3 x 4.0  | 5         | 5000        | 30             |
|             |               | PSO  | TC 114.3 x 6.4  | TC 114.3 x 4.0  | TC 101.6 x 4.5  | 6         | 5000        | 35             |

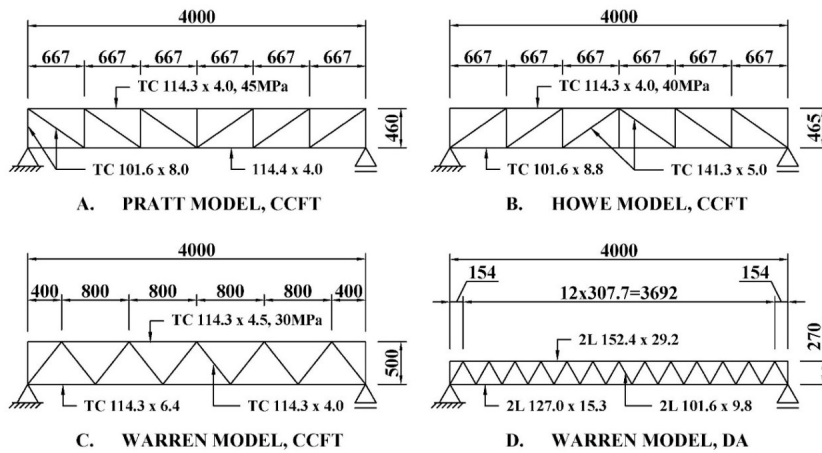


**Figure 10.** Final geometry to the best solutions to the 40-m truss.

It is possible to notice, as in the previous examples, that there is a clear tendency of solutions using DA to use more panels and lower heights, in order to minimize the size of the elements. Three of the 6 solutions using DA reached the lower bound of the search interval considered, while two of the solutions for CCFT reached the upper bound. Figure 11 shows the best solutions between GA and PSO for each case, in relation to the best solution.

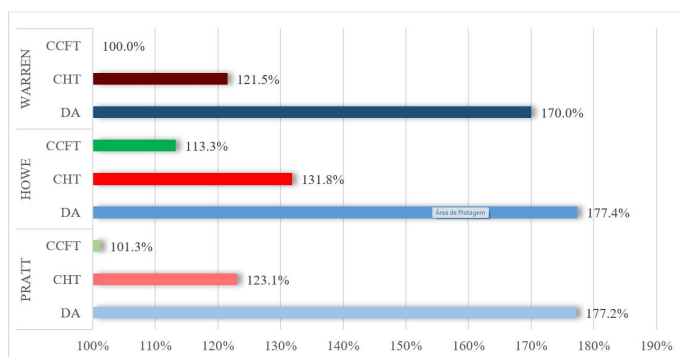


**Figure 11 -** Comparison between solutions provided to the 40-m truss.

Once again following the tendency, the Warren truss using CCFT was the most efficient solution and the Howe truss using DA the least efficient, a difference even greater than the one found in previous examples, reaching 77.4%. It was found that the trusses using CHT emits, on average, 19.81% more CO<sub>2</sub> than the ones using CCFT, a value that is even higher for trusses using DA, where the average emission is 67.24% higher. Figure 12 shows the reduction of total CO<sub>2</sub> emission obtained by substituting DA profiles by CHT and CCFT in each example.

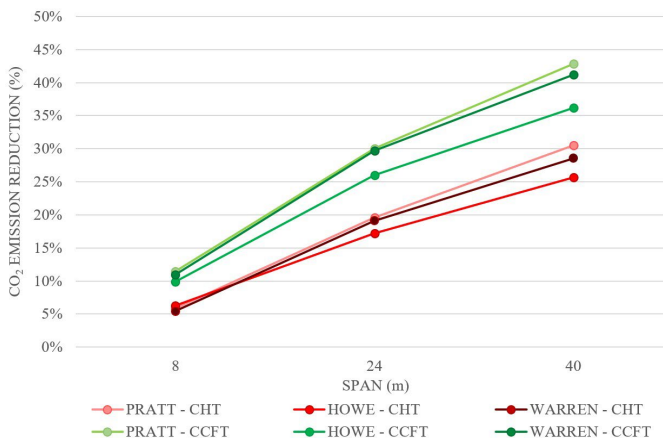


Figure 12 - CO<sub>2</sub> Emission reduction in relation to the DA solution.

It is possible to conclude that, the greater the span, the greater the reduction obtained by using CCFT instead of DA. That can be better explained by Figure 13, which shows the detailed emission caused by each element of the truss. In it, profiles are shown to be the largest responsible for the total emission of the beam, in contrast to the previous examples, where its representativeness was quite inferior.

In this case it is possible to notice that steel profiles are the largest responsible for the CO<sub>2</sub> emission of all solutions, reaching more than two thirds of the entire emission, in the case of DA trusses. The steel shape follows as the second largest emitter and the concrete slab the next. As the dimensions of the profiles of the upper chord increased, the emission due to the filling concrete now exceeds the emission of the connectors, with more than 1%, but with a value still derisory when compared to the substantial savings caused by the reduction in the steel weight of profiles. Table 10 shows the relation between design and resistant efforts to each of the safety criteria analyzed and Figure 14 presents an analysis of the constraints.

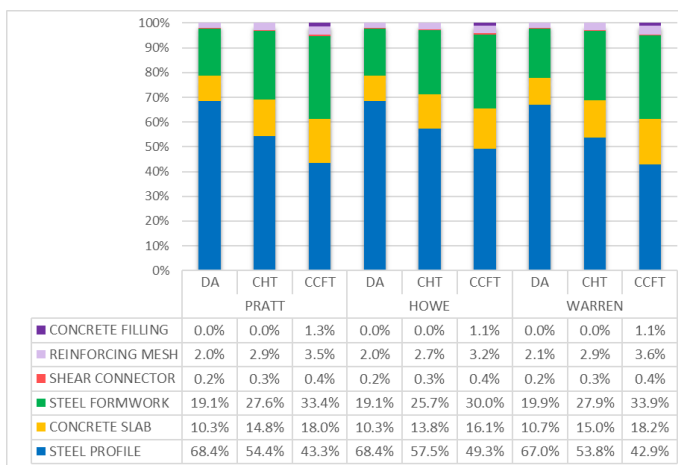
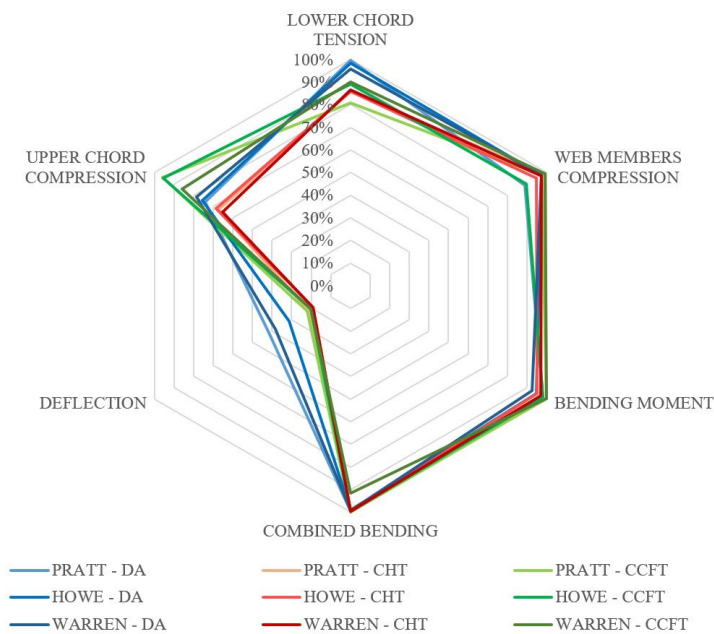


Figure 13. CO<sub>2</sub> Emission Composition of a 40-m span truss.

**Table 10** - Relation between design and resistant efforts of the solutions.

| Truss Model | Profile Shape | Upper Chord Compression | Lower Chord Tension | Web Members Compression | Bending Moment | Combined Bending | Deflection |
|-------------|---------------|-------------------------|---------------------|-------------------------|----------------|------------------|------------|
| Pratt       | DA            | 74.09%                  | 99.55%              | 88.79%                  | 98.05%         | <b>99.67%</b>    | 41.76%     |
|             | CHT           | 67.35%                  | 86.04%              | 98.09%                  | <b>99.84%</b>  | 98.66%           | 21.45%     |
|             | CCFT          | 95.67%                  | 80.69%              | 97.47%                  | 99.85%         | <b>99.90%</b>    | 22.10%     |
| Howe        | DA            | 75.44%                  | 98.45%              | 97.55%                  | 94.95%         | <b>99.22%</b>    | 31.39%     |
|             | CHT           | 68.55%                  | 85.90%              | 94.91%                  | 95.10%         | <b>99.87%</b>    | 18.92%     |
|             | CCFT          | 95.35%                  | 89.17%              | 89.82%                  | 98.26%         | <b>99.62%</b>    | 20.34%     |
| Warren      | DA            | 78.42%                  | 95.80%              | 97.53%                  | 92.59%         | <b>99.39%</b>    | 38.16%     |
|             | CHT           | 65.21%                  | 86.67%              | 97.21%                  | 97.12%         | <b>99.70%</b>    | 18.94%     |
|             | CCFT          | 85.85%                  | 90.11%              | 99.24%                  | <b>99.88%</b>  | 91.52%           | 20.36%     |



**Figure 14.** Constraints analysis provided to the 40-m truss.

By analyzing Table 10 and Figure 14, it is noted that the bending moment and combined bending were the determinant criteria in the dimensioning of all solutions. It is also noticed that the lower chord tension was more critical for trusses using DA, while the compression in the upper chord approached closer to the resistance limit in the trusses using CCFT, indicating a better exploitation of the elements when using concrete filling.

#### 4. CONCLUSIONS

By analyzing the results obtained for each algorithm in the three examples studied, it was possible to notice that both converged to equal or similar solutions. For the first case, where the span was smaller, all the solutions provided were the same for both algorithms. For the other case, where the spans were larger, most results diverged. The divergence between the algorithms tested, however, did not exceed 2% in any case, confirming the effectiveness of the solutions. In general, the PSO was more efficient than the GA in obtaining the best solutions to the problems analyzed.

As for the models of truss, it was concluded that the most effective model for the cases analyzed was Warren, followed by Pratt and, finally, Howe. Among the profile shapes, the trusses using DA were the least efficient, followed by trusses using CHT and CCFT being the most efficient. The overall emission saving varied, being even more significant for longer span lengths, much because the use of this type of section reduced the weight of the profiles, which are the major responsible for the general emission of the truss in these cases. The saving provided by filling the upper chord was 5.4% in the 8-meter span example and reached almost 20% for the 40-meter span. Comparing the

solutions using CHT and CCFT, it was concluded that the increase in emission caused by the filling concrete is much lower than the emission avoided by the reduction of profiles weight.

In all examples, the best solutions were to concrete with  $f_{ck}$  equal 20MPa for the slab, but the same did not happen for the concrete fillings of the CCFT profiles. The choice of concrete used in the slab, as well as steel formwork and reinforcement mesh, did not vary, indicating that these parameters are not influenced by the span size. The strength of the filling concrete, on the other hand, varied between span lengths and truss models, but all the best solutions were found for concretes with compressive strength equal to or greater than 25 MPa. These results reinforce that, although concretes with higher resistances generate a higher CO<sub>2</sub> emission, their use allowed for a general gain in resistance that helped minimize the use of steel and, consequently, the total emission of the truss.

Regarding the constraints that governed the analyzed problems, the combined bending criterion was critical in the optimum design of all examples, generating a design-resistant relation greater than 90% in all cases. Another critical criterion in many cases, especially in solutions using tubular profiles, was the bending moment. In the trusses of the solutions using DA, in general, the criterion of lower chord tension was more relevant, while the upper chord compression was more relevant in the solutions using CCFT. In all the solutions, the governing criterion reached more than 96% in the relation between design and resistant efforts, confirming the efficiency of the optimization algorithm.

## 5. ACKNOWLEDGEMENTS

The authors are thankful to the Brazilian Federal Government Agency CAPES for the financial support provided during the development of this research. The second author thanks the Brazilian Federal Government Agency CNPq for the productivity research grant number 309741/2020-3.

## 6. REFERENCES

- [1] Intergovernmental Panel on Climate Change, *Contribution of Working Groups I, II and III to the Fourth Assessment Report on Intergovernmental Panel on Climate Change: Climate Change 2007: Synthesis Report*, Geneva, IPCC, 2007.
- [2] Intergovernmental Panel on Climate Change, *Contribution of Working Group II to the Sixth Assessment Report of the Intergovernmental Panel on Climate Change: Climate Change 2022: Impacts, Adaptation, and Vulnerability*, Cambridge, Cambridge University Press, 2022.
- [3] UN Environment and International Energy Agency, *2020 Global Status Report for Buildings and Construction: Towards a Zero-Emission, Efficient, and Resilient Buildings and Construction Sector*, Nairobi, United Nations Environment Programme, 2021.
- [4] I. Payá-Zaforteza, V. Yepes, A. Hospitaler, and F. González-Vidosa, "CO<sub>2</sub>-optimization of reinforced concrete frames by simulated annealing," *Eng. Struct.*, vol. 31, no. 7, pp. 1501–1508, 2009, <http://dx.doi.org/10.1016/j.engstruct.2009.02.034>.
- [5] D. Yeo and R. D. Gabbai, "Sustainable design of reinforced concrete structures through embodied energy optimization," *Energy Build.*, vol. 43, pp. 2028–2033, 2011, <http://dx.doi.org/10.1016/j.enbuild.2011.04.014>.
- [6] V. Yepes, F. Gonzalez-Vidosa, J. Alcalá, and P. Villalba, "CO<sub>2</sub>-optimization design of reinforced concrete retaining walls based on a VNS-threshold acceptance strategy," *J. Comput. Civ. Eng.*, vol. 26, no. 3, pp. 378–386, 2012, [http://dx.doi.org/10.1061/\(asce\)cp.1943-5487.0000140](http://dx.doi.org/10.1061/(asce)cp.1943-5487.0000140).
- [7] C. V. Camp and F. Huq, "CO<sub>2</sub> and cost optimization of reinforced concrete frames using a big bang-big crunch algorithm," *Eng. Struct.*, vol. 48, pp. 363–372, 2013, <http://dx.doi.org/10.1016/j.engstruct.2012.09.004>.
- [8] G. F. de Medeiros and M. Kripka, "Optimization of reinforced concrete columns according to different environmental impact assessment parameters," *Eng. Struct.*, vol. 59, pp. 185–194, 2014, <http://dx.doi.org/10.1016/j.engstruct.2013.10.045>.
- [9] S. W. Choi, B. K. Oh, J. S. Park, and H. S. Park, "Sustainable design model to reduce environmental impact of building construction with composite structures," *J. Clean. Prod.*, vol. 137, pp. 823–832, 2016, <http://dx.doi.org/10.1016/j.jclepro.2016.07.174>.
- [10] T. Dede, M. Kripka, V. Togan, V. Yepes, and R. V. Rao, "Usage of optimization techniques in civil engineering during the last two decades," *Curr. Trends Civ. Struct. Eng.*, vol. 2, no. 1, 2019, <http://dx.doi.org/10.33552/ctcse.2019.02.000529>.
- [11] A. F. Tormen, Z. M. C. Pravia, F. B. Ramires, and M. Kripka, "Optimization of steel concrete composite beams considering cost and environmental impact," *Steel Compos. Struct.*, vol. 34, no. 3, pp. 409–421, 2020, <http://dx.doi.org/10.12989/scs.2020.34.3.409>.
- [12] N. D. Lagaros, "The environmental and economic impact of structural optimization," *Struct. Multidiscipl. Optim.*, vol. 58, no. 4, pp. 1751–1768, 2018, <http://dx.doi.org/10.1007/s00158-018-1998-z>.
- [13] B. K. Oh, S. W. Choi, and H. S. Park, "Influence of variations in CO<sub>2</sub> emission data upon environmental impact of building construction," *J. Clean. Prod.*, vol. 140, pp. 1194–1203, 2017, <http://dx.doi.org/10.1016/j.jclepro.2016.10.041>.
- [14] M. M. Khasreen, P. F. G. Banfill, and G. F. Menzies, "Life-cycle assessment and the environmental impact of buildings: a review," *Sustainability*, vol. 1, no. 3, pp. 674–701, 2009, <http://dx.doi.org/10.3390/su1030674>.

- [15] T. García Segura and V. Yepes, "Multiobjective optimization of post-tensioned concrete box-girder road bridges considering cost, CO2 emissions, and safety," *Eng. Struct.*, vol. 125, pp. 325–336, 2016, <http://dx.doi.org/10.1016/j.engstruct.2016.07.012>.
- [16] J. F. Santoro and M. Kripka, "Minimizing environmental impact from optimized sizing of reinforced concrete elements," *Comput. Concr.*, vol. 25, no. 2, pp. 111–118, 2020, <http://dx.doi.org/10.12989/cac.2020.25.2.111>.
- [17] A. A. A. Esmín, R. A. Coelho, and S. Matwin, "A review on particle swarm optimization algorithm and its variants to clustering high-dimensional data," *Artif. Intell. Rev.*, vol. 44, no. 1, pp. 23–45, 2015, <http://dx.doi.org/10.1007/s10462-013-9400-4>.
- [18] V. Govindaraj and J. V. Ramasamy, "Optimum detailed design of reinforced concrete continuous beams using Genetic Algorithms," *Comput. Struct.*, vol. 84, no. 1–2, pp. 34–48, 2005, <http://dx.doi.org/10.1016/j.compstruc.2005.09.001>.
- [19] C. A. C. Coello, A. D. Christiansen, and F. S. Hernández, "A simple genetic algorithm for the design of reinforced concrete beams," *Eng. Comput.*, vol. 13, no. 4, pp. 185–196, 1997, <http://dx.doi.org/10.1007/bf01200046>.
- [20] V. K. Koumousis and S. J. Arsenis, "Genetic algorithms in optimal detailed design of reinforced concrete members," *Comput. Civ. Infrastruct. Eng.*, vol. 13, no. 1, pp. 43–52, 1998, <http://dx.doi.org/10.1111/0885-9507.00084>.
- [21] B. D. Breda, T. C. Pietralonga, and E. C. Alves, "Optimization of the structural system with composite beam and composite slab using Genetic Algorithm," *IBRACON Struct. Mater. J.*, vol. 13, no. 6, pp. 1–14, 2020, <http://dx.doi.org/10.1590/s1983-41952020000600002>.
- [22] A. H. Whitworth and K. D. Tsavdaridis, "Genetic algorithm for embodied energy optimisation of steel-concrete composite beams," *Sustainability*, vol. 12, no. 8, pp. 1–17, 2020, <http://dx.doi.org/10.3390/SU12083102>.
- [23] A. B. Senouci and M. S. Al-Ansari, "Cost optimization of composite beams using genetic algorithms," *Adv. Eng. Softw.*, vol. 40, no. 11, pp. 1112–1118, 2009, <http://dx.doi.org/10.1016/j.advengsoft.2009.06.001>.
- [24] F. Erdal, E. Doan, and M. P. Saka, "Optimum design of cellular beams using harmony search and particle swarm optimizers," *J. Construct. Steel Res.*, vol. 67, no. 2, pp. 237–247, 2011, <http://dx.doi.org/10.1016/j.jcsr.2010.07.014>.
- [25] G. Erlacher and E. C. Alves, "Optimal design of composite cellular beams with partial interaction and its environmental impacts", in *ABMEC-IACM*, Rio de Janeiro, 2021.
- [26] R. E. Perez and K. Behdinan, "Particle swarm optimization in structural design," in *Swarm Intelligence, Focus on Ant and Particle Swarm Optimization*, F. T. Chan, M. K. Tiwari, Eds., London, United Kingdom: IntechOpen, 2007, pp. 373–394.
- [27] A. C. C. Lemonge and H. J. C. Barbosa, "An adaptive penalty scheme for genetic algorithms in structural optimization," *Int. J. Numer. Methods Eng.*, vol. 59, no. 5, pp. 703–736, 2004, <http://dx.doi.org/10.1002/nme.899>.
- [28] A. Baghlani and M. H. Makiabadi, "An enhanced particle swarm optimization for design of pin connected structures," *Sci. Iran.*, vol. 20, no. 5, pp. 1415–1432, 2013.
- [29] F. B. Ramires, S. A. L. Andrade, P. C. G. S. Vallasco, and L. R. O. Lima, "Genetic algorithm optimisation of composite and steel endplate semi-rigid joints," *Eng. Struct.*, vol. 45, pp. 177–191, 2012, <http://dx.doi.org/10.1016/j.engstruct.2012.05.051>.
- [30] J. Wardenier, Y. Kurobane, J. A. Packer, D. Dutta, and N. Yeomans, *Design Guide for Circular Hollow Section (CHT) Joints Under Predominantly Static Loading*. Germany: Comité International pour le Développement et l'Étude de la Construction Tubulaire, 1991.
- [31] S. A. Raji, K. K. Abdulraheem, R. O. Rahmon, and A. A. Adelowo, "Design of a composite truss system in a multistorey building," *J. Multidiscip. Eng. Sci. Technol.*, vol. 4, no. 3, pp. 6863–6870, 2017.
- [32] J. Bujnak, P. Michalek, and W. Baran, "Experimental and theoretical investigation of composite truss beams", in *MATEC Web Conference*, 2018, vol. 174, pp. 6–13, <https://doi.org/10.1051/mateconf/201817404001>.
- [33] J. D. Martins, S. E. Pereira, E. M. Jr., Xavier, L. H. A. Neiva, and A. M. C. Sarmanho, "Experimental and numerical analysis of composite steel and concrete trusses," *IBRACON Estruturas Mater. J.*, vol. 14, pp. 1–14, 2021, <http://dx.doi.org/10.1590/s1983-41952021000200001>.
- [34] A. Kaveh and B. Ahmadi, "Sizing, geometry and topology optimization of trusses using force method and supervised charged system search," *Struct. Eng. Mech.*, vol. 50, 2014, <http://dx.doi.org/10.12989/sem.2014.50.3.365>.
- [35] M. A. K. Tarabay and L.S. Lima, "Otimização topológica, geométrica e dimensional de estruturas metálicas treliçadas, dimensionadas conforme a norma ABNT NBR 8800: 2008," *REA*, vol. 11, pp. 21–38, 2022.
- [36] T. E. Müller and E. van der Klashorst, "A quantitative comparison between size, shape, topology and simultaneous optimization for truss structures," *Lat. Am. J. Solids Struct.*, vol. 14, no. 12, pp. 2221–2242, 2017, <http://dx.doi.org/10.1590/1679-78253900>.
- [37] Gerdau. "Perfis estruturais Gerdau: tabela de bitolas." <https://mais.gerdau.com.br/catalogos-e-manuais/> (accessed Apr. 26, 2022).
- [38] Vallourec Tubos do Brasil. "Tubos estruturais de seção circular, quadrada e retangular." <https://www.aecweb.com.br/empresa/vallourec/20437/downloads/1> (accessed Apr. 26, 2022).
- [39] METFORM. "Catálogo de Fôrmas." [www.aecweb.com.br](http://www.aecweb.com.br) (accessed Apr. 26, 2022).
- [40] Worldsteel Association. "LCI data for steel products." <https://worldsteel.org> (accessed May 27, 2022).
- [41] Associação Brasileira de Normas Técnicas, *Design of steel and composite steel and concrete structures for buildings*, ABNT NBR 8800, 2008.

- [42] Associação Brasileira de Normas Técnicas, *Design of steel and composite structures for buildings using hollow sections*, ABNT NBR 16239, 2013.
- [43] Associação Brasileira de Normas Técnicas, *Cargas para o cálculo de estruturas de edificações*, ABNT NBR 6120, 2019.
- [44] S. A. Guimarães, D. Klein, A. F. G. Calenzani, and E. C. Alves, "Optimum design of steel columns filled with concrete via genetic algorithm: environmental impact and cost analysis," *REM Int. Eng. J.*, vol. 75, no. 1, pp. 117–128, 2022, <http://dx.doi.org/10.1590/0370-44672021750034>.
- [45] J. S. Lourenção, P. A. T. Arpini, G. Erlacher, and E. C. Alves, "Optimized design of concrete-filled steel columns," *IBRACON Struct. Mater. J.*, vol. 15, no. 1, pp. e15102, 2022, <http://dx.doi.org/10.1590/s1983-41952022000100002>.

---

**Author contributions:** GE: formal analysis, data curation, writing; AFGC: formal analysis, data curation, writing, supervision; ECA: methodology, formal analysis, data curation, conceptualization, writing, supervision.

**Editors:** Edna Possan, Guilherme Aris Parsekian.